THE JOURNAL OF PHYSICAL CHEMISTRY C

ARTICLE

pubs.acs.org/JPCC

# Open-Circuit Voltage Limitation in Low-Bandgap Diketopyrrolopyrrole-Based Polymer Solar Cells Processed from Different Solvents

Pablo P. Boix,[†] Martijn M. Wienk,[‡] René A. J. Janssen,[‡] and Germà Garcia-Belmonte*[,†]

[†]Photovoltaic and Optoelectronic Devices Group, Departament de Física, Universitat Jaume I, ES-12071 Castelló, Spain

[‡]Molecular Materials and Nanosystems, Department of Applied Physics and Department of Chemical Engineering and Chemistry, Eindhoven University of Technology, P.O. Box 513, 5600 MB Eindhoven, The Netherlands

Supporting Information

**ABSTRACT:** Low-bandgap diketopyrrolopyrrole-based polymer bulk-heterojunction solar cells prepared from different solvents are studied by means of capacitance measurements. Large variations of both photovoltage and photocurrent are induced during device processing by using different solvents that allow internal operating energetics to be addressed. Addition of *o*-dichlorobenzene to chloroform produces an upward offset of the polymer highest occupied molecular orbital level in accordance with the red shift of the absorption spectra, which correlates with the flat-band potential offset extracted from Mott−Schottky analysis of the reverse and low-forward capacitance. However, the open-circuit voltage does not reach the expected value in the case of chloroform-processed devices because of the reduced occupancy of the acceptor fullerene lower unoccupied molecular orbital states extracted from the chemical capacitance analysis under illumination. This photovoltage loss is linked with the limitation to the increase in the electron Fermi level caused by the reduced charge density involved in the photovoltaic process, as derived from the morphology-influenced short-circuit current density.

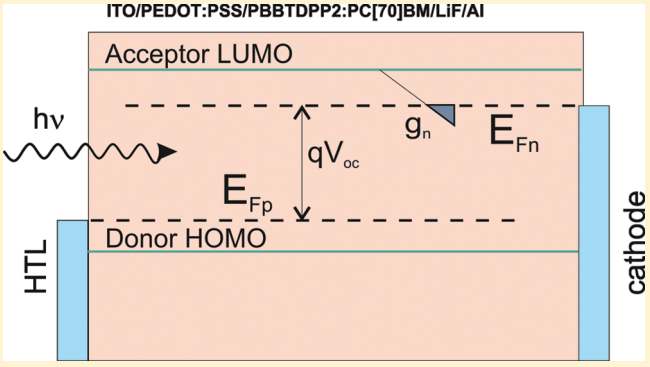


## 1. INTRODUCTION

With the aim of improving organic solar cell power conversion efficiencies (PCE), there has been extensive work on the design and synthesis of low-bandgap polymers with extended absorption onset into the infrared region, thereby enhancing light harvesting. One of the most promising organic families contains diketopyrrolopyrrole-based (DPP) units as absorber building blocks. Very recently, the combination of DPP-based polymers or oligomers and [6,6]phenyl-$C_{71}$-butyric acid methyl ester ($PC_{70}BM$) has been used in organic solar devices exhibiting PCE within the range of 3.5−5.5%.[1−5] Apart from narrowing the optical bandgap, PCE increases by tailoring the energetic position of the donor highest occupied molecular orbital (HOMO), because it plays a crucial role in establishing the reachable open-circuit voltage $V_{oc}$.[6] It has been demonstrated in addition that the actual location of the donor HOMO level is highly dependent on the solar cell processing procedure.[1] For instance, the blend of the narrow-bandgap polymer poly[3,6-bis(4′-dodecyl[2,2′-bithiophen]-5-yl)-2,5-bis(2-ethylhexyl)-2,5-dihydropyrrolo[3,4-*c*]-pyrrole-1,4-dione] (PBBTDPP2) and [6,6]phenyl-$C_{61}$-butyric acid methyl ester ($PC_{60}BM$) was reported to exhibit a photovoltaic performance that changes with the solvent used during preparation: spin-coated films from chloroform show photovoltage with a 1 sun illumination ($V_{oc}$ = 0.78 V) and optical gap values (1.7 eV) higher than those observed when the chloroform/*o*-dichlorobenzene (ODCB) mixture is used ($V_{oc}$ = 0.63 V and optical gap of 1.4 eV).[1] Such qualitative correlation between $V_{oc}$ and light absorption onset suggests that the polymer HOMO level experiences an energy shift by effect of the used solvent, but the displacement of $V_{oc}$ only approximately reaches half of the absorption red shift, thus indicating that some kind of energy loss occurs that limits the increase in the open-circuit voltage. $V_{oc}$ limitation could have different origins: from (i) a partial shift of the polymer HOMO to (ii) a downward displacement of the acceptor lower unoccupied molecular orbital (LUMO) to (iii) a reduced occupancy of the fullerene LUMO that limits the increase of the electron Fermi level. We will next demonstrate that it is the third possibility that actually occurs in these solar devices.

To gain greater insight into the role of the donor HOMO and acceptor LUMO positions on the operating energetic of polymer/fullerene solar cells, we will next identify the relevant energy levels for the device performance by using a purely electrical technique based on capacitance measurements, following the method reported recently.[7] The performance of solar cells comprising PBBTDPP2/$PC_{70}BM$ blends, prepared from chloroform and mixed chloroform/ODCB solvents as described in

**Received:** April 8, 2011
**Revised:** May 23, 2011

   dx.doi.org/10.1021/jp203279f | *J. Phys. Chem. C* XXXX, XXX, 000–000

previous work,[1] is compared and analyzed using capacitive methods both in the dark (Mott−Schottky analysis) and under illumination and open-circuit conditions. We finally relate the photovoltage loss to the reduced charge density involved in the photovoltaic process for chloroform-processed cells.

## 2. RESULTS AND DISCUSSION

Solar cells with an indium tin oxide (ITO)/poly(3,4-ethylenedioxythiophene):poly(styrene sulfonic acid) (PEDOT:PSS)/PBBTDPP2:$PC_{70}BM$/LiF/Al structure, prepared from chloroform and mixed chloroform/ODCB solvents, were described in previous work.[1] Capacitance and impedance measurements were performed with Autolab PGSTAT-30 equipped with a frequency analyzer module. The AC oscillating amplitude was as low as 20 mV (rms) to maintain the linearity of the response (see the Supporting Information for fitting details). Measurements were performed in the dark at different bias voltages, and under zero-current conditions by applying a bias that equals $V_{oc}$ under varying continuous irradiation conditions.[8]

An example of the measured current−density voltage ($J-V$) characteristics under simulated AM1.5G illumination (1000 $W/m^2$) of PBBTDPP2:$PC_{70}BM$ solar cells is plotted in Figure 1. We systematically observed that $V_{oc}$ at 1 sun illumination is higher for cells processed with only chloroform than for cells for which the solvent contains ODCB and chloroform (see Table 1), as also observed for $PC_{60}BM$-processed devices.[1] This difference ($\Delta V_{oc}$) attains values approximately equal to 0.18 V. The short-circuit current $J_{sc}$ always exhibits larger values for devices processed from a mixed choloform/ODCB solution (4:1) then increasing the power conversion efficiency. The shift in $V_{oc}$ has been attributed to the less negative PBBTDPP2 HOMO position caused by the electronic interaction among the polymer chains, which is present upon introduction of ODCB.[1] Such an effect is qualitatively in good agreement with the experimentally observed correlation between the donor HOMO and acceptor LUMO difference (effective gap of the blend), and the open-circuit voltage as $qV_{oc} \propto E_{LUMO}(A) - E_{HOMO}(D)$, $q$ being the elementary charge.[6] However, the measured $\Delta V_{oc}$ is lower than that expected from the red shift (from 720 to 860 nm, i.e., ∼0.3 eV) at the onset of the absorption and EQE spectra previously reported.[1] At this point, it is unknown whether the optical gap change is produced by displacements of both donor HOMO and LUMO levels or solely caused by the HOMO offset. We will next demonstrate that it is actually the second case that occurs (HOMO offset) by processing with different solvents. As we will next see, a decrease in $V_{oc}$ will be related to a limitation in the acceptor LUMO occupancy, rather than to a partial shift of the donor HOMO.

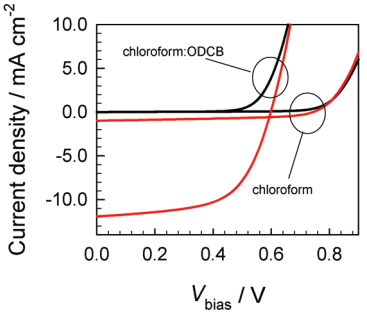


**Figure 1.** Current density−voltage characteristics of typical ITO/PEDOT:PSS/PBBTDPP2:$PC_{70}BM$/LiF/Al devices processed with chloroform and choloform/ODCB solvents.

To improve our understanding of the difference in open-circuit voltage $V_{oc}$, we have performed capacitance−voltage $C-V$ measurements in the dark, which is known to provide information about contact energetics.[9] Here we interpret the $C-V$ measurements in terms of the voltage modulation of the free carrier depletion zone made up in the vicinity of the contact.[10] The capacitance in reverse and low-forward bias relates to the width of the depletion zone, which changes via variation of the applied voltage. Such a depletion zone appears as a consequence of the doped character of the polymer. Inherent energetic disorder of organic semiconductors resulting from structural inhomogeneities or chemical impurities enhances charge localization and gives rise to carrier trapping. Negatively charged defects (acceptor states) donate a hole to the transport-related HOMO levels and are then responsible for the p-doping of the polymer. An illustrative band diagram is depicted in Figure 2: before contact is made, there exists an energy level offset between the doped polymer $\phi_s$ and the contact $\phi_c$. Here $\phi_s = E_{F0}$ stands for the polymer/fullerene work function (Fermi level), which is located near the polymer HOMO level because of the p-doping, and $\phi_c$ corresponds to the contact work function as in Figure 2a,b. As a consequence of the absence of electronic $\pi-\pi$ interactions between the polymer chains, the polymer HOMO level is located at a more negative position when chloroform is used as solvent. It is assumed in addition that the cathode work function is determined by LiF/Al. After contact is made, the band bending compensates for the work function mismatch, and such a difference relates to the flat-band potential as $qV_{fb} = \phi_c - \phi_s$, as shown in the equilibrium conditions in Figure 2c,d. It is assumed that the anodes always form ohmic contacts by aligning $E_{F0}$ to the HOMO of the hole transporting and conductive PEDOT:PSS layer. Negatively charged defects form an immobile space charge zone exhibiting a voltage-dependent width. This kind of contact usually exhibits Mott−Schottky characteristics ($C^{-2} \propto V$),[8,11,12] which has been readily interpreted as a strong indication of the presence of acceptor defect levels within the polymer energy gap. Alternative techniques like Kelvin probe[13] and ultraviolet photoelectron spectroscopy[14] have provided further evidence of the formation of depletion zones at metal−organic contacts with the corresponding band bending caused by the presence of impurity levels.

Figure 3a shows $C-V$ characteristics measured at a low frequency (100 Hz). At reverse bias, the capacitance saturates to the geometrical value $C_g = \varepsilon\varepsilon_0/L \approx 37$ nF/$cm^2$ (where $L$ is for the active layer thickness, $\varepsilon_0$ the permittivity of the vacuum, and $\varepsilon$ the dielectric constant), because the active layer reaches full depletion. Variations of $C_g$ within 20% are encountered among different cells related to layer thickness and permittivity changes.

**Table 1. Photovoltaic Parameters and Results from the Mott−Schottky Analysis of PBBTDPP2:$PC_{70}BM$ Solar Cells**

| | $J_{sc}$ (mA/$cm^2$) | $V_{oc}$ (V) | FF | PCE (%) | $V_{fb}$ (V) | $N$ ($\times 10^{16}$ $cm^{-3}$) |
|---|---|---|---|---|---|---|
| chloroform | 1.0 | 0.78 | 0.51 | 1.4 | 0.84 | 3.07 |
| chloroform/ODCB (4:1) | 11.9 | 0.60 | 0.58 | 4.0 | 0.48 | 3.43 |


dx.doi.org/10.1021/jp203279f | J. Phys. Chem. C XXXX, XXX, 000–000

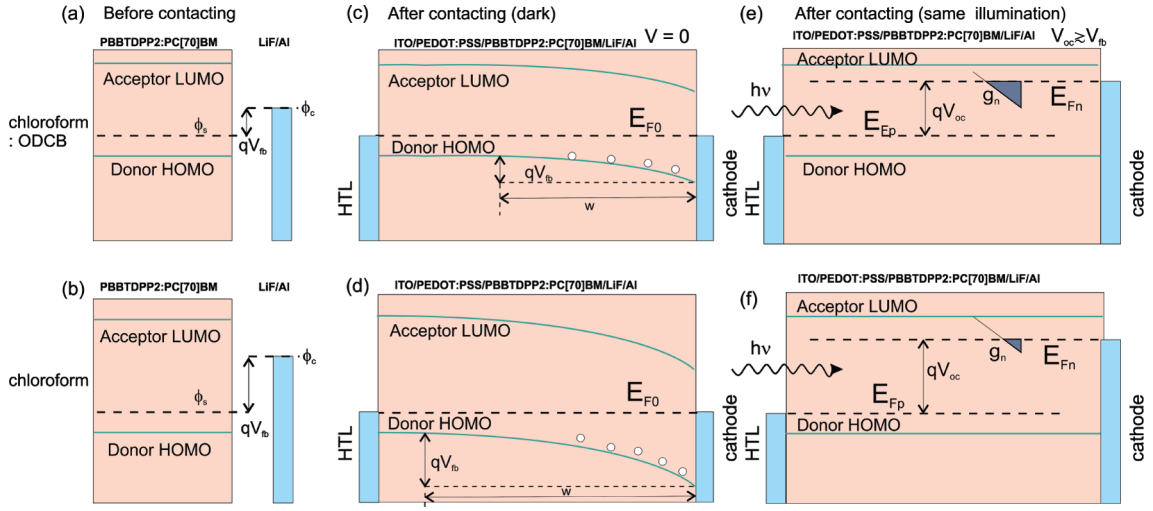


**Figure 2.** Energy diagram representing donor HOMO and acceptor LUMO levels, the active layer work function $\phi_s$, and the LiF/Al cathode work function $\phi_c$, for structures processed with the choloform/ODCB mixture (a) and choloform alone (b) before contact is made. $\phi_s$ is positioned closer to the donor HOMO because of a higher level of doping. The distance between acceptor LUMO and cathode work function is the same, whereas the donor HOMO is shifted. (c and d) Band diagram of a p-doped donor polymer−acceptor fullerene blend at zero bias voltage (in the dark). A depletion zone of width $w$ is formed at the cathode, and an ohmic contact at the hole transporting PEDOT:PSS layer (HTL) interface. The work function offset ($V_{fb}$) produces a band bending by Fermi level alignment $E_{F0}$. (e and f) Band diagram under illumination, and open-circuit conditions producing $V_{oc} \geq V_{fb}$. The Fermi level splitting accounts for $V_{oc}$. The electron occupation of the fullerene LUMO levels (filled area of $g_n$) is different because of the reduced charge carrier density involved in the case of chloroform-processed samples. In all the diagrams, the same energy scale is adopted.

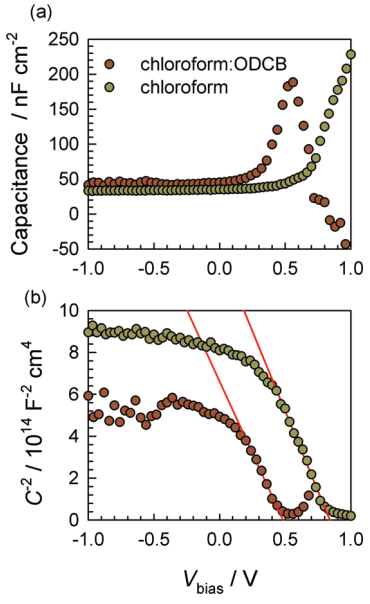


**Figure 3.** (a) Comparison of the capacitance−voltage response of chloroform- and choloform/ODCB mixture-processed devices. Capacitance measured in the dark at room temperature and 100 Hz. (b) Mott−Schottky characteristics $[C^{-2}(V)]$ of the solar cells exhibiting a linear relationship (straight lines) at forward bias and a plateau at reverse signaling full-depleted active layers.

In any case, the dielectric constant $\varepsilon$ always lies within the range of 3−4. To verify that the analyzed devices actually exhibit Mott−Schottky characteristics, the capacitance as $C^{-2}(V)$ is shown versus the applied voltage in Figure 3b. A linear relationship is observed at low forward voltages, with the intercept with the voltage axis being related to the flat-band potential $V_{fb}$. The density of defect states $N$ (p-doping of the organic layer) is derived from the linear slope by means of the Mott−Schottky relation

$$C^{-2} = \frac{2(V_{fb} - V)}{q\varepsilon\varepsilon_0 N} \quad (1)$$

where $N$ is the total concentration of negatively charged defects (see Table 1), which establishes the dark hole density $p_0 = N$. The total density under dark conditions results in $N \approx 3 \times 10^{16}$ cm$^{-3}$ for both kinds of cells, which indicates that both active layers are doped to the approximately same extent despite the observed shift in the polymer HOMO position. Because the doping level is similar, the energy distance between the polymer HOMO level and the Fermi level $E_{F0}$ is not altered by ODCB addition, as illustrated in Figure 2.

It also important to note that full depletion (equaling the active layer thickness of 100 nm) is reached at a reverse bias of approximately 0.4 V, by using the values in Table 1 to calculate the depletion layer width $\{w = [2\varepsilon\varepsilon_0(V_{fb} - V)/qN]^{1/2}\}$. Via examination of Figure 3b, one can observe that deviations from the linear Mott−Schottky relation of eq 1 appear at forward bias (∼0.2 V for mixed solvent-processed samples). There is then a voltage range from 0.2 to −0.4 V within which the transition to full depletion is rather smooth. The progress of the limit of the depletion zone approaching the anode is determined by the actual doping profile. The dopant spatial distribution might vary in real devices because of vertical phase segregation giving rise to $C^{-2}(V)$ shapes that deviate from the simpler linear form in eq 1. Overall, an estimation of the doping level in the vicinity of the cathode can be made via selection of the adequate voltage range.

It is observed that the main difference between both samples is the large offset in $V_{fb}$. A $\Delta V_{fb}$ of 0.36 V that relates to the displacement of the HOMO level of the polymer is found. As drawn in Figure 2, the addition of ODCB produces an upward offset of the PBBTDPP2 HOMO level in accordance with the red


dx.doi.org/10.1021/jp203279f |J. Phys. Chem. C XXXX, XXX, 000–000

shift (~0.3 eV) of the absorption spectra.[1] We note that such a 0.36 V upward shift of the HOMO level is also in accordance with cyclic voltammetry signals of PBBTDPP2 in an ODCB solution. In ODCB, PBBTDPP2 is partly aggregated and shows two consecutive onsets of oxidation for aggregated and fully dissolved chains that are 0.27 eV apart (see the Supporting Information). Polymer aggregation then stabilizes energy levels by moving them upward, causing both the observed red shift and the offset in $V_{fb}$. As pointed out in previous work, it is the perturbation of the HOMO and LUMO levels produced by aggregation or crystallinity after blending that actually lies behind values of the open-circuit voltage achieved in devices.[15]

A general device operating picture (Figure 2c,d) draws upon consideration of a band bending at the cathode that scales with the polymer HOMO energy. As discussed previously, such a HOMO level offset does not alter the relative position of the Fermi energy with respect to the polymer HOMO, as derived from the similar doping encountered. Importantly, it is observed that $V_{fb}$ scales with the PBBTDPP2 HOMO level, and it is much smaller than the built-in voltage $V_{bi}$ resulting from the work function difference between the ITO/PEDOT and LiF/Al contacts ($V_{bi} \approx 1$ V). Therefore, $V_{fb}$ appears to be a distinctive feature of the cathode, forming the anode ohmic contact (Figure 2c,d). We highlight the fact that $C-V$ measurements in combination with absorption experiments provide complete information about the polymer HOMO and LUMO level location.

After observing that the $\Delta V_{fb}$ of 0.36 V correlates with the ~0.3 eV red shift of the absorption spectra, we would have expected similar changes in $V_{oc}$, because the polymer HOMO displacement should affect both $V_{fb}$ and $V_{oc}$ by the same amount. We notice, however, that $\Delta V_{oc} = 0.18$ V. To uncover the reasons behind this discrepancy, we next need to introduce the relation between the output open-circuit voltage and the charge carrier Fermi levels under illumination. In every solar cell, the open-circuit photovoltage that can be achieved by a given material or blend is equal to the difference between the electron and hole chemical potentials (quasi-Fermi levels) in the absorbing layer under steady-state illumination.[16,17]

$$qV_{oc} = E_{Fn} - E_{Fp} \tag{2}$$

Hence, the output voltage measured under open-circuit conditions monitors the splitting of the Fermi levels, which in turn are stated by the charge carrier concentrations. This idea is drawn in Figure 2e,f, where $qV_{oc}$ amounts to the free energy distance between carrier (electron and hole) Fermi levels. Because of the p-doping character of the polymer, the downward shift of $E_{Fp}$ via the effect of illumination should be restricted within a few $k_BT$ (thermal energy), as $E_{F0} - E_{Fp} \approx k_BT \ln(\Delta p/p_0)$. This is because the amount of excess, photogenerated holes for usual illumination intensities of around 1 sun, lies within an order of magnitude of the density of dopants ($p_0 \approx \Delta p = 10^{16}-10^{17}$ cm$^{-3}$).[18] Photogeneration then moves the electron Fermi level $E_{Fn}$ upward while slightly displacing the hole Fermi level downward. As a consequence, $E_{Fp}$ acts as an energy reference for $V_{oc}$.

When the band bending vanishes at $V \approx V_{fb}$, we expect that the device capacitance is governed by a chemical capacitance due to the excess of minority carriers $C_\mu$,[8,16] which is related to the change in the occupancy of electrons in the LUMO of the fullerene, as follows

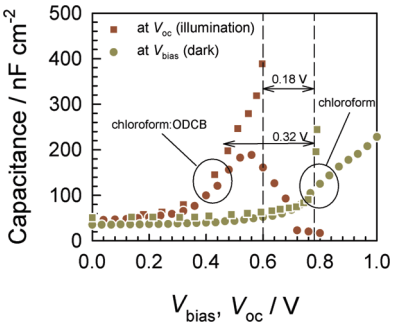


**Figure 4.** Comparison of depletion zone capacitance as in Figure 3a and the chemical capacitance $C_\mu$ extracted from impedance spectroscopy analysis under open-circuit conditions under varying illumination intensities. The increase in $C_\mu$ at $V_{oc} \geq V_{fb}$ points to the filling of fullerene LUMO DOS. A voltage shift of ~0.32 V is encountered between the DOS manifolds that relates to the displacement of the PBBTDPP2 HOMO level ($\Delta V_{fb} = 0.36$ V). Dashed vertical lines correspond to $V_{oc}$ values achieved at a 1 sun illumination intensity with each type of cell. A $\Delta V_{oc}$ of 0.18 V is found to be lower than $\Delta V_{fb}$.

$$C_\mu = q^2 L \frac{dn}{dE_{Fn}} \tag{3}$$

Here the capacitance is given per unit area, and $n$ corresponds to the electron concentration. The chemical capacitance is in fact a representation of the electron density of states (DOS) as $C_\mu = q^2 L g_n(V_{oc})$.[8,15,19] According to eq 3, the capacitance should increase with the forward bias as the DOS occupancy progresses. However, the measured capacitance in Figure 3 exhibits a decrease at forward bias, which eventually develops a negative value at large forward bias for samples processed with the choloform/ODCB mixture. We notice that the negative capacitance effect appears under operating conditions in which a dc current is allowed to flow.[20] Recently, we have proposed a measuring procedure of the capacitance at different illumination intensities,[8] to avoid the negative response in the capacitance. The applied bias voltage compensates for the effect of the photovoltage, so that effectively the cell is measured under open-circuit conditions; i.e., the photogeneration current is canceled by the charge recombination flow, and $J_{dc} = 0$. Such measuring conditions have the additional effect of assuring a homogeneous distribution of charge carriers along the active layer. A comparison of the chemical capacitance (under open-circuit conditions under varying illuminations) and the depletion layer capacitance (in the dark under varying bias) is drawn in Figure 4. By examining this plot, we observe that the capacitance exceeds the depletion layer capacitive values at $V_{oc} \geq V_{fb}$. This entails that the proposed experimental method allows for a direct measurement of the chemical capacitance.[7]

The filling of fullerene LUMO levels starts at larger open-circuit voltages in the case of chloroform-processed devices. This is viewed as a voltage shift in Figure 4 of ~0.32 V, which approximately coincides with the difference in flat-band potential between these cells. Regardless of the voltage shift, the similar shape of the $C_\mu(V_{oc})$ plot in Figure 4 suggests that the same acceptor LUMO states are being monitored. The DOS extracted from $C_\mu$ exhibits an approximate exponential form as $g_n(V_{oc}) \propto \exp(\alpha q V_{oc}/k_BT)$ with $\alpha \approx 0.14$, indicating a large DOS tail with


dx.doi.org/10.1021/jp203279f | J. Phys. Chem. C XXXX, XXX, 000–000

a characteristic energy near 180 meV.[15] Moreover, the absolute energy position of the fullerene LUMO is observed to be unaltered, but the acceptor LUMO occupation achieves different levels at 1 sun illumination as derived from the difference in chemical capacitance values resulting for samples processed with the choloform/ODCB mixture ($C_\mu$ = 390 nF/cm$^2$) in comparison with a $C_\mu$ of 196 nF/cm$^2$ for samples processed with chloroform alone (see Figure 4). We then observe that the shifts in flat-band potential and the onset of $PC_{70}BM$ LUMO occupancy are correlated, because it is actually the hole Fermi level $E_{Fp}$ that takes the role of the energy reference in both cases, as depicted in Figure 2e,f. In this diagram, the cathode contact Fermi level follows the rise of $E_{Fn}$ via the effect of illumination, starting from $E_{F0}$ in the dark, as explained previously.[7,20] This means that the cathode work function does not actually pin $V_{oc}$ as observed experimentally.[15,21]

We now return to the remaining question of the $V_{oc}$ offset. It is demonstrated that both $V_{fb}$ and $C_\mu(V_{oc})$ displacements (~0.32−0.36 V) correlate with the offset of the PBBTDPP2 HOMO level as derived from the red shift of the absorption spectra. However, the $V_{oc}$ difference at 1 sun is lower than expected (0.18 V). The open-circuit voltage increment and flat band shift are expected to be similar ($\Delta V_{oc} \approx \Delta V_{fb}$) only in those cases in which the increase in $E_{Fn}$ attains comparable values, as stated in eq 2. We then attribute the difference ($\Delta V_{fb} - \Delta V_{oc}$ = 0.18 V) to a relatively lower position of $E_{Fn}$ in the case of chloroform-processed samples (see Figure 2e,f), rather than a shift of the fullerene LUMO level, for a similar (1 sun) illumination intensity. The lower position of $E_{Fn}$ informs on the reduced charge density involved in the photovoltaic process in the case of chloroform-based devices. We notice here that the lower charge density that is responsible for the reduced photovoltage also can be inferred from the different short-circuit current density levels encountered (see Table 1). Addition of ODCB to the solvent increases $J_{sc}$ by approximately 1 order of magnitude. This has been attributed to a morphological effect: while layers from the chloroform/ODCB mixture exhibit more uniform structures with only small features (<100 nm), films from chloroform contain domains with lateral dimensions of several hundreds of nanometers.[1] It has been suggested that large fullerene domains act as electron drains reducing the observed photocurrent.[22] Because the short-circuit current scales virtually linearly with light intensity, a light intensity of 0.1 sun brings the ODCB-processed cell to the same level of charge generation as the chloroform cell under 1 sun. At 0.1 sun, the reduction in $V_{oc}$ is ~0.08 V for the cell processed with ODCB ($\Delta V_{oc}$ + 0.08 V = 0.26 V), in qualitative agreement with the absorption red shift and flat-band offset of ~0.3 V. This last observation entails that the photogeneration current is voltage-independent, giving rise to $J_{sc}$ under short-circuit conditions, and equaling the charge carrier recombination current under open-circuit conditions. Remarkably, phase-separated large domains within the active layers are then responsible for the reduced extent of generation of charges, which lies behind both the lower photocurrent and the lower than expected photovoltage of chloroform-processed devices.

## 3. CONCLUSIONS

We have presented a coherent picture describing the operating energetics of diketopyrrolopyrrole-based bulk-heterojunction solar cells. The addition of ODCB produces an upward offset of the PBBTDPP2 HOMO level in accordance with the red shift of the absorption, which correlates with $\Delta V_{fb}$. The key point is the observation that the hole Fermi level $E_{F0}$ determines the flat-band potential, extracted from the usual Mott−Schottky analysis of the reverse and low-forward capacitance. We have also pointed out that the actual $E_{F0}$ position is linked to the amount of negatively charged defects that donates holes to the polymer HOMO levels, then displacing $E_{F0}$ downward and approaching the HOMO manifold. Moreover, $E_{F0}$ acts as an energy reference for $V_{oc}$. Finally, the open-circuit voltage difference does not reach the expected values because of the limited occupancy of the fullerene LUMO levels, which do not undergo significant shifts, in the case of chloroform-processed devices. This photovoltage loss is linked with the reduced charge density involved in the photovoltaic process as derived from the morphology-influenced short-circuit current density.

## ■ ASSOCIATED CONTENT

**Supporting Information.** Cyclic voltammetry signal of PBBTDPP2 processed from a mixed choloform/ODCB solvent (Figue S1), the equivalent circuit used to fit impedance spectra (Figure S2), and an example of impedance spectra registered under open-circuit conditions at different white light illumination intensities (Figure S3). This material is available free of charge via the Internet at http://pubs.acs.org.

## ■ AUTHOR INFORMATION

**Corresponding Author**

*E-mail: garciag@fca.uji.es. Telephone: +34 964 387548. Fax: +34 964 729218.

## ■ ACKNOWLEDGMENT

We are thankful for financial support from Ministerio de Educacion y Ciencia under Project HOPE CSD2007-00007 (Consolider-Ingenio 2010) and Generalitat Valenciana (Prometeo/2009/058, ACOMP/2009/056, and ACOMP/2009/095). P.P.B. acknowledges an ESF short-visit grant (3083).

## ■ REFERENCES

(1) Wienk, M. M.; Turbiez, M.; Gilot, J.; Janssen, R. A. J. Narrow-Bandgap Diketo-pyrrolo-pyrrole Polymer Solar Cells: The Effect of Processing on the Performance. *Adv. Mater.* **2008**, *20*, 2556–2560.

(2) Walker, B.; Tamayo, A. B.; Dang, X.-D.; Zalar, P.; Seo, J. H.; Garcia, A.; Tantiwiwat, M.; Nguyen, T.-Q. Nanoscale Phase Separation and High Photovoltaic Efficiency in Solution-Processed, Small-Molecule Bulk Heterojunction Solar Cells. *Adv. Funct. Mater.* **2009**, *19*, 3063–3069.

(3) Huo, L.; Hou, J.; Chen, H. Y.; Zhang, S.; Jiang, Y.; Chen, T. L.; Yang, Y. Bandgap and Molecular Level Control of the Low-Bandgap Polymers Based on 3,6-Dithiophen-2-yl-2,5-dihydropyrrolo[3,4-c]-pyrrole-1,4-dione toward Highly Efficient Polymer Solar Cells. *Macromolecules* **2009**, *42*, 6564–6571.

(4) Bijleveld, J. C.; Gevaerts, V. S.; Nuzzo, D. D.; Turbiez, M.; Mathijssen, S. G. J.; Leeuw, D. M. d.; Wienk, M. M.; Janssen, R. A. J. Efficient Solar Cells Based on an Easily Accessible Diketopyrrolopyrrole Polymer. *Adv. Mater.* **2010**, *22*, E242–E246.

(5) Jo, J.; Gendron, D.; Najari, A.; Moon, J. S.; Cho, S.; Leclerc, M.; Heeger, A. J. Bulk Heterojunction Solar Cells Based on a Low-Bandgap Carbazole-Diketopyrrolopyrrole Copolymer. *Appl. Phys. Lett.* **2010**, *97*, 203303.

(6) Scharber, M.; Mühlbacher, D.; Koppe, M.; Denk, P.; Waldauf, C.; Heeger, A. J.; Brabec, C. J. Design Rules for Donor Bulk-

Heterojunction Solar Cells-Towards 10% Energy-Conversion Efficiency. *Adv. Mater.* **2006**, *18*, 789–794.

(7) Boix, P. P.; Ajuria, J.; Etxebarria, I.; Pacios, R.; Garcia-Belmonte, G.; Bisquert, J. Role of ZnO Electron-Selective Layers in Regular and Inverted Bulk Heterojunction Solar Cells. *J. Phys. Chem. Lett.* **2011**, *2*, 407–411.

(8) Garcia-Belmonte, G.; Boix, P. P.; Bisquert, J.; Sessolo, M.; Bolink, H. J. Simultaneous Determination of Carrier Lifetime and Electron Density-of-States in P3HT:PCBM Organic Solar Cells under Illumination by Impedance Spectroscopy. *Sol. Energy Mater. Sol. Cells* **2010**, *94*, 366–375.

(9) Mensfoort, S. L. M. v.; Coehoorn, R. Determination of Injection Barriers in Organic Semiconductor Devices from Capacitance Measurements. *Phys. Rev. Lett.* **2008**, *100*, 086802.

(10) Sze, S. M. *Physics of Semiconductor Devices*, 2nd ed.; John Wiley and Sons: New York, 1981.

(11) Limpinsel, M.; Wagenpfahl, A.; Mingebach, M.; Deibel, C.; Dyakonov, V. Photocurrent in Bulk Heterojunction Solar Cells. *Phys. Rev. B* **2010**, *81*, 085203.

(12) Seemann, A.; Sauermann, T.; Lungenschmied, C.; Armbruster, O.; Bauer, S.; Egelhaaf, H.-J.; Hauch, J. Reversible and Irreversible Degradation of Organic Solar Cell Performance by Oxygen. *Sol. Energy* **2011**, *85*, 1238–1249.

(13) Ishii, H.; Hayashi, N.; Ito, E.; Washizu, Y.; Sugi, K.; Kimura, Y.; Niwano, M.; Ouchi, Y.; Seki, K. Kelvin Probe Study of Band Bending at Organic Semiconductor/Metal Interfaces: Examination of Fermi Level Alignment. *Phys. Status Solidi A* **2004**, *201*, 1075–1094.

(14) Nishi, T.; Kanai, K.; Ouchi, Y.; Willis, M. R.; Seki, K. Evidence for the Atmospheric p-Type Doping of Titanyl Phthalocyanine Thin Film by Oxygen Observed as the Change of Interfacial Electronic Structure. *Chem. Phys. Lett.* **2005**, *414*, 479–482.

(15) Garcia-Belmonte, G.; Boix, P. P.; Bisquert, J.; Lenes, M.; Bolink, H. J.; La Rosa, A.; Filippone, S.; Martín, N. Influence of the Intermediate Density-of-States Occupancy on Open-Circuit Voltage of Bulk Heterojunction Solar Cells with Different Fullerene Acceptors. *J. Phys. Chem. Lett.* **2010**, *1*, 2566–2571.

(16) Bisquert, J.; Cahen, D.; Hodes, G.; Rühle, S.; Zaban, A. Physical Chemical Principles of Photovoltaic Conversion with Nanoparticulate, Mesoporous Dye-Sensitized Solar Cells. *J. Phys. Chem. B* **2004**, *108*, 8106–8118.

(17) Garcia-Belmonte, G.; Bisquert, J. Open-Circuit Voltage Limit Caused by Recombination through Tail States in Bulk Heterojunction Polymer-Fullerene Solar Cells. *Appl. Phys. Lett.* **2010**, *96*, 113301.

(18) Maurano, A.; Hamilton, R.; Shuttle, C. G.; Ballantyne, A. M.; Nelson, J.; O'Regan, B.; Zhang, W.; McCulloch, I.; Azimi, H.; Morana, M.; Brabec, C. J.; Durrant, J. R. Recombination Dynamics as a Key Determinant of Open Circuit Voltage in Organic Bulk Heterojunction Solar Cells: A Comparison of Four Different Donor Polymers. *Adv. Mater.* **2010**, *22*, 4987–4992.

(19) Sánchez-Díaz, A.; Izquierdo, M.; Filippone, S.; Martín, N.; Palomares, E. The Origin of the High Voltage in DPM12/P3HT Organic Solar Cells. *Adv. Funct. Mater.* **2010**, *20*, 2695–2700.

(20) Bisquert, J. A variable Series Resistance Mechanism to Explain the Negative Capacitance Observed in Impedance Spectroscopy Measurements of Nanostructured Solar Cells. *Phys. Chem. Chem. Phys.* **2011**, *13*, 4679–4685.

(21) Lenes, M.; Wetzelaer, G.-J. A. H.; Kooisrta, F. B.; Veenstra, S. C.; Hummelen, J. C.; Blom, P. W. M. Fullerene Bisadducts for Enhanced Open-Circuit Voltages and Efficiencies in Polymer Solar Cells. *Adv. Mater.* **2008**, *20*, 2116–2119.

(22) Maturová, K.; van Bavel, S. S.; Wienk, M. M.; Janssen, R. A. J. Morphological Device Model for Organic Bulk Heterojunction Solar Cells. *Nano Lett.* **2009**, *9*, 3032–3037.